

Fabrication and electrochemical performances of single crystal $\text{LiNi}_{0.91}\text{Co}_{0.06}\text{Mn}_{0.03}\text{O}_2$ cathode material via heat-treatment

In-Ho Im^a and Seung-Hwan Lee^{b,*}

^aDepartment of Electrical Engineering, Shin Ansan University, Republic of Korea

^bDepartment of Advanced Materials Engineering, Daejeon University, Daejeon 34520, Republic of Korea

We successfully synthesized a single crystal $\text{LiNi}_{0.91}\text{Co}_{0.06}\text{Mn}_{0.03}\text{O}_2$ via heat-treatment and measured its electrochemical performances. The structural characterizations and electrochemical properties of single crystal $\text{LiNi}_{0.91}\text{Co}_{0.06}\text{Mn}_{0.03}\text{O}_2$ are studied in order to apply to lithium-ion batteries for electric vehicles. The crystallization and morphology of the sample are measured by XRD, SEM. An initial discharge capacity of single crystal $\text{LiNi}_{0.91}\text{Co}_{0.06}\text{Mn}_{0.03}\text{O}_2$ is 202.1 mAh g^{-1} . Also it exhibits superior capacity retention of 89.7% under high current density of 4.0 C, which are higher electrochemical performances as compared to previously reported polycrystalline sample. Therefore, we can conclude that single crystal $\text{LiNi}_{0.91}\text{Co}_{0.06}\text{Mn}_{0.03}\text{O}_2$ can be regarded as an effective way for next generation cathode candidate.

Keywords: Single crystal $\text{LiNi}_{0.91}\text{Co}_{0.06}\text{Mn}_{0.03}\text{O}_2$, Heat treatment, Electrochemical performances, Next generation cathode candidate.

Introduction

Lithium-ion batteries are the most widely used energy storage devices around the world. It is applied to electric vehicles, hybrid vehicles, new and renewable energy, data storage centers, etc. It can be explained by high energy density of lithium-ion batteries. Currently, various studies are being conducted to improve the poor life characteristics, safety, and power density, which are pointed out as shortcomings of lithium ion batteries [1, 2].

Doping, coating, shape control, etc. are being studied using commercially available polycrystalline materials, but there are limitations to improve the disadvantages of polycrystalline by itself. In order to overcome the drawbacks of polycrystalline and obtain excellent electrochemical performance, the research trend has recently changed to manufacture a single crystal cathode. This is because the particles of single crystal become bigger than those of polycrystalline, which results in a lower specific surface area [3].

As a method of manufacturing a single crystal, heat treatment, sol-gel method, hydrothermal synthesis method, etc. are widely reported. Among them, the heat treatment method is the simplest method because it can prepare single crystal using a polycrystalline material as a starting material [4, 5].

In this paper, we successfully prepared and single crystal $\text{LiNi}_{0.91}\text{Co}_{0.06}\text{Mn}_{0.03}\text{O}_2$ and measured structural

properties and electrochemical performances to confirm the possibility of polycrystalline substitution.

Experimental

For superior electrochemical performances, single crystal $\text{LiNi}_{0.91}\text{Co}_{0.06}\text{Mn}_{0.03}\text{O}_2$ powders were prepared via using co-precipitation method. The $\text{Ni}_{0.91}\text{Co}_{0.06}\text{Mn}_{0.03}(\text{OH})_2$ precursor was prepared using aqueous solution of $\text{NiSO}_4 \cdot 6\text{H}_2\text{O}$, $\text{CoSO}_4 \cdot 7\text{H}_2\text{O}$, $\text{MnSO}_4 \cdot \text{H}_2\text{O}$, Na_2CO_3 and $\text{NH}_3 \cdot \text{H}_2\text{O}$. Precipitating agent was prepared using the NH_4OH and NaOH solution, simultaneously. The spherical precursor blended with $\text{LiOH} \cdot \text{H}_2\text{O}$ (molar ratio of Li and precursor was 1.05 : 1). Afterward, the mixture was calcined at $700 \text{ }^\circ\text{C}$ for 5 h and then sintered $850 \text{ }^\circ\text{C}$ for 15 h in O_2 atmosphere, as shown in Fig. 1.

For electrochemical tests, the cathode was fabricated via active material powder (96 wt%), Super P (2 wt%) and polyvinylidene fluoride (PVDF) binder (2 wt%). In order to form slurry, N-methyl-pyrrolidinone (NMP) solvent was mixed. Subsequently, slurry was coated on Al-foil and dried at $120 \text{ }^\circ\text{C}$ for 10 h in a vacuum oven to remove the NMP solvent. The CR 2032 coin cells were fabricated with Li foil as an anode in argon-gas filled glove box. 1M LiPF_6 in ethylene carbonate (EC), dimethyl carbonate (DMC) and ethyl methyl carbonate (EMC) (with a volumetric ratio 1 : 1 : 1) were selected as an electrolyte.

For structural properties and morphologies, X-ray diffraction (XRD, X'pert MPD DY1219) and field emission scanning electron microscopy (FE-SEM, Hitachi S-4800) were used. The initial charge-discharge capacities and long-term cycle performances are measured by

*Corresponding author:
Tel : +82-42-280-2414
E-mail: shlee@dju.kr

electrochemical equipment (TOSCAT-3100, Toyo system).

Results and Discussion

The crystallinity of single crystal $\text{LiNi}_{0.91}\text{Co}_{0.06}\text{Mn}_{0.03}\text{O}_2$ powders is investigated by X-ray diffraction (XRD) spectra and the 2θ angle is scanned in the range of $10 - 70^\circ$, as shown in Fig. 2. According to the XRD spectra results, single crystal $\text{LiNi}_{0.91}\text{Co}_{0.06}\text{Mn}_{0.03}\text{O}_2$ can be indexed to $\alpha\text{-NaFeO}_2$ layered structure belonging to the $R\bar{3}m$ space group without any impurity phases [1]. It indicates that lithium ions are on the 3a sites (lithium layer), transition metals (TM) are on the 3b sites (TM layer) and oxygen ions are on the 6c sites [2]. Moreover, the peak splitting of the Miller indices (006)/(102) and (108)/(110) pairs in single crystal $\text{LiNi}_{0.91}\text{Co}_{0.06}\text{Mn}_{0.03}\text{O}_2$ is clearly divided which contributes to the characteristic of crystal structure [3]. Also, the I_{003}/I_{104} ratio of single crystal $\text{LiNi}_{0.91}\text{Co}_{0.06}\text{Mn}_{0.03}\text{O}_2$ is 1.49, which is higher than 1.2 exhibits a well-ordered layer structure without obvious cation mixing [4, 5]. It indicates that unwanted cation mixing does not take place and single crystal $\text{LiNi}_{0.91}\text{Co}_{0.06}\text{Mn}_{0.03}\text{O}_2$ has a well-ordered layered structure [6]. In other words, the high I_{003}/I_{104} in single crystal $\text{LiNi}_{0.91}\text{Co}_{0.06}\text{Mn}_{0.03}\text{O}_2$ can be translated as a suppressed cation mixing crystal structure [7]. The cation mixing

is occurred due to the similar radius between Ni^{2+} (0.79 Å) and Li^+ (0.76 Å) [6]. Moreover, the full-width half maximum (FWHM) values of (003) peak is 0.18° . The peak of (104) reflection between $K\alpha_1$ and $K\alpha_2$ in the SCNCM is narrow. The calculated FWHM values of the (104) peak of single crystal $\text{LiNi}_{0.91}\text{Co}_{0.06}\text{Mn}_{0.03}\text{O}_2$ is small (0.21°), suggesting that single crystal $\text{LiNi}_{0.91}\text{Co}_{0.06}\text{Mn}_{0.03}\text{O}_2$ has enlarged particle size [8].

The microstructure of single crystal $\text{LiNi}_{0.91}\text{Co}_{0.06}\text{Mn}_{0.03}\text{O}_2$ is displayed in Fig. 3. The single crystal $\text{LiNi}_{0.91}\text{Co}_{0.06}\text{Mn}_{0.03}\text{O}_2$ has large primary particles in the size of $1.1 - 2.9 \mu\text{m}$. It is well known that polycrystalline sample exhibits micrometer-sized secondary particles by the aggregation of numerous nano-sized primary particles. The most noteworthy changes of single crystal $\text{LiNi}_{0.91}\text{Co}_{0.06}\text{Mn}_{0.03}\text{O}_2$ is grain boundary. Unlike polycrystalline, single crystal $\text{LiNi}_{0.91}\text{Co}_{0.06}\text{Mn}_{0.03}\text{O}_2$ has smooth surface morphology and little grain boundaries. The big particle size with smooth surface can decrease the contact area between the cathode material and the electrolyte, which leads to the reduction of negative reaction thereby improving the electrochemical performances [1, 9].

Fig. 4 shows the initial charge and discharge voltage profiles of single crystal $\text{LiNi}_{0.91}\text{Co}_{0.06}\text{Mn}_{0.03}\text{O}_2$ in the voltage range of 3.0-4.3 V at 0.5 C rate ($1 \text{ C} = 200 \text{ mAhg}^{-1}$). The single crystal $\text{LiNi}_{0.91}\text{Co}_{0.06}\text{Mn}_{0.03}\text{O}_2$ has

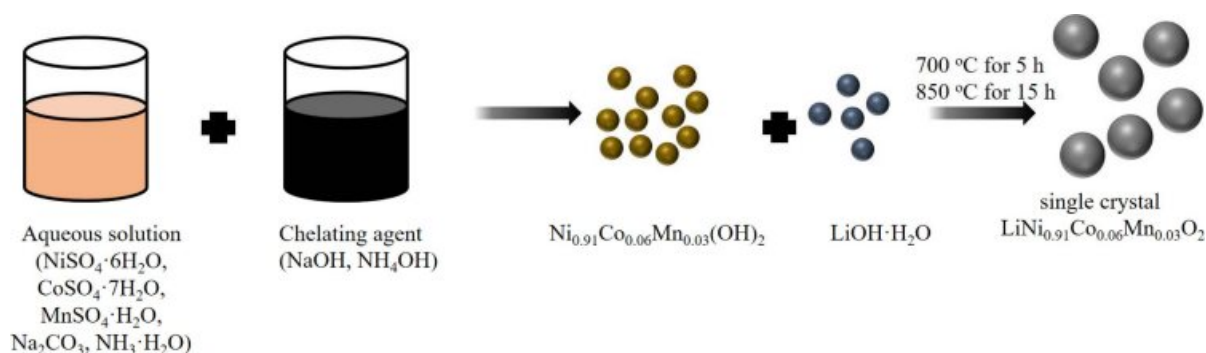


Fig. 1. Schematic illustration of the synthesis process of single crystal $\text{LiNi}_{0.91}\text{Co}_{0.06}\text{Mn}_{0.03}\text{O}_2$.

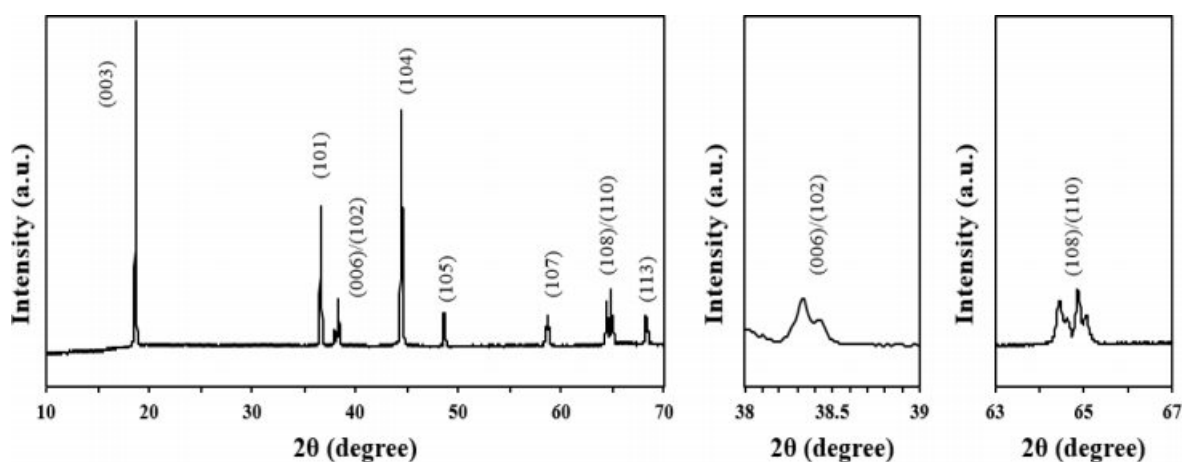


Fig. 2. XRD pattern of single crystal $\text{LiNi}_{0.91}\text{Co}_{0.06}\text{Mn}_{0.03}\text{O}_2$.

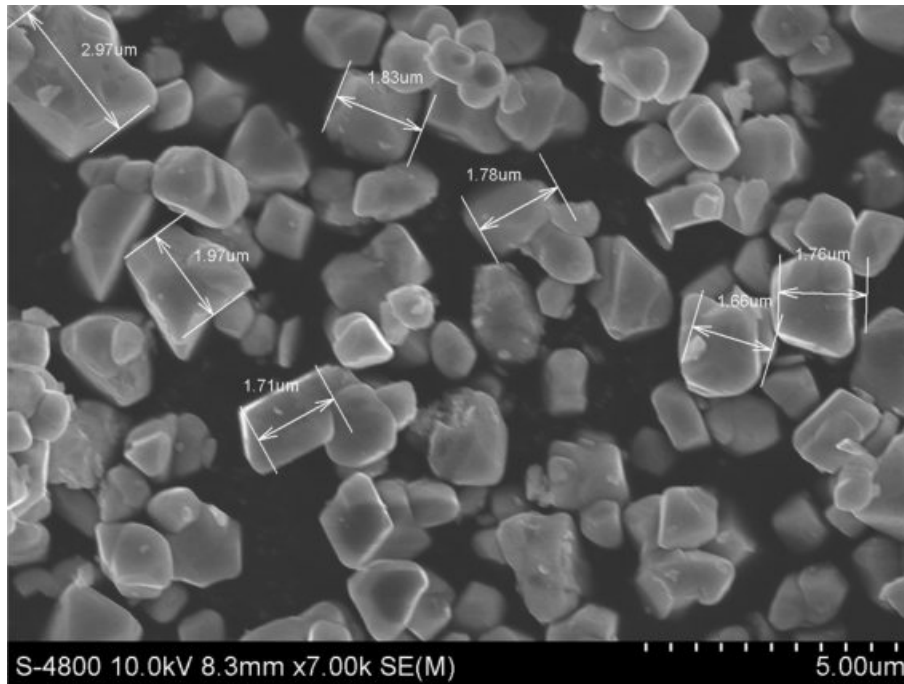


Fig. 3. FESEM image of single crystal $\text{LiNi}_{0.91}\text{Co}_{0.06}\text{Mn}_{0.03}\text{O}_2$.

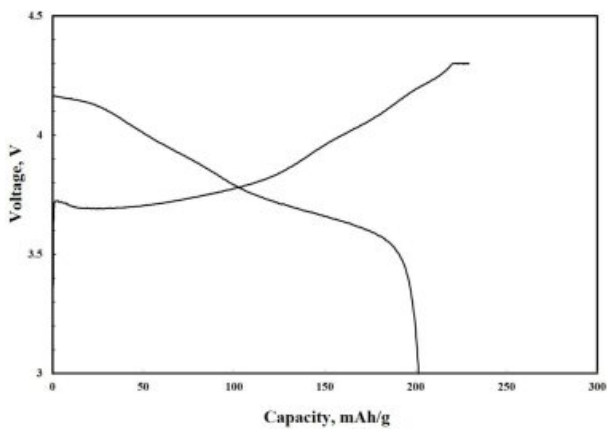


Fig. 4. Initial charge-discharge profile of single crystal $\text{LiNi}_{0.91}\text{Co}_{0.06}\text{Mn}_{0.03}\text{O}_2$.

a typical potential plateau. The first charge/discharge capacities of single crystal $\text{LiNi}_{0.91}\text{Co}_{0.06}\text{Mn}_{0.03}\text{O}_2$ are 219.8 mAhg^{-1} and 202.1 mAhg^{-1} , respectively with the coulombic efficiency of 91.9%. The irreversible capacity loss of single crystal $\text{LiNi}_{0.91}\text{Co}_{0.06}\text{Mn}_{0.03}\text{O}_2$ is inevitable in Ni-rich ternary cathode materials owing to surface instability and parasitic reaction, such as oxidative electrolyte decomposition, during long-term cycling [10, 11]. However, higher discharge capacity and coulombic efficiency in single crystal $\text{LiNi}_{0.91}\text{Co}_{0.06}\text{Mn}_{0.03}\text{O}_2$ can be elucidated that stable surface chemistry of micro-sized particles facilitates the Li-ion intercalation-deintercalation [1, 2]. On the contrary, it is well known that the polycrystalline demonstrates decay of voltage plateau with increasing cycles, indicating severe structural degradation [11].

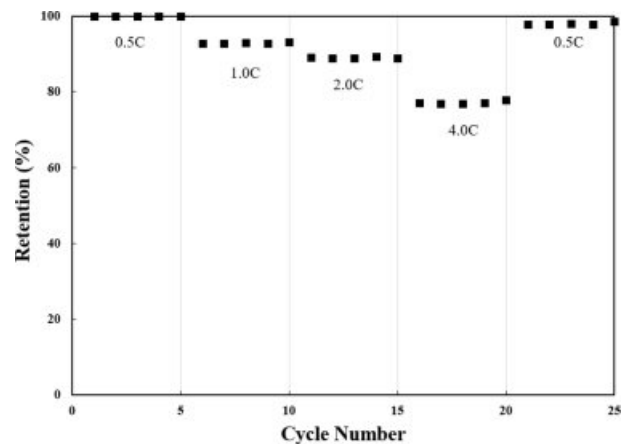


Fig. 5. Rate performance of single crystal $\text{LiNi}_{0.91}\text{Co}_{0.06}\text{Mn}_{0.03}\text{O}_2$.

The rate performance testes at different current densities ranging from 0.5 C to 4.0 C are shown in Fig. 5. The retentions of single crystal $\text{LiNi}_{0.91}\text{Co}_{0.06}\text{Mn}_{0.03}\text{O}_2$ are declined with increasing C-rate, which is ascribed to sluggish lithium ion kinetics. The retentions of single crystal $\text{LiNi}_{0.91}\text{Co}_{0.06}\text{Mn}_{0.03}\text{O}_2$ are 99.9, 93.5, 89.7 and 77.9% at 0.5 C, 1.0, 2.0 and 4.0 C, respectively, which are superior capacity retention compared to previously reported polycrystalline [12]. Even at high current rate of 4C, the single crystal $\text{LiNi}_{0.91}\text{Co}_{0.06}\text{Mn}_{0.03}\text{O}_2$ maintains the original layered structure. Moreover, the single crystal $\text{LiNi}_{0.91}\text{Co}_{0.06}\text{Mn}_{0.03}\text{O}_2$ recovered about 99.1% of its initial capacity when the current density returned to 0.5 C again. This is because enhanced surface chemical and structural stability of single-crystalline, originated from significantly reduced unwanted reactions.

Consequently, this results in rapid and reversible electrochemical kinetics [6, 8].

Conclusions

Single crystal $\text{LiNi}_{0.91}\text{Co}_{0.06}\text{Mn}_{0.03}\text{O}_2$ is successfully prepared via annealing treatment. The single crystal $\text{LiNi}_{0.91}\text{Co}_{0.06}\text{Mn}_{0.03}\text{O}_2$ sample delivers good cyclability and rate performance as well as initial charge-discharge capacities compared to previously reported polycrystalline. It can be inferred that the specific surface area of single crystal $\text{LiNi}_{0.91}\text{Co}_{0.06}\text{Mn}_{0.03}\text{O}_2$ is relatively smaller than that of polycrystalline sample. It could significantly decrease in unfavorable side reaction between liquid electrolyte and cathode by strengthen surface chemistry. As a result, it was confirmed that heat treatment, which is the simplest and easiest method and can realize superior electrochemical performances, is a very effective single crystal manufacturing method.

Acknowledgements

This work was supported by the National Research Foundation of Korea (NRF) grant funded by the Korea government (MSIT) (No. 2021R1F1A1055979).

References

1. Y. Lv, X. Cheng, W. Qiang, B. Huang, J. Power Sources. 450 (2020) 227718.
2. S.J. Sim, S.H. Lee, B.S. Jin, H.S. Kim, Sci. Rep. 9 (2019) 8952.
3. L. Tang, Y. Liu, H. Wei, C. Yan, Z.J. He, Y.J. Li, J.C. Zheng, J. Energy Chem. 55 (2021) 114-123.
4. Z. Peng, G. Yang, F. Li, Z. Zhu, Z. Liu, J. Alloy. Comp. 762 (2018) 827-834.
5. G. Hu, Y. Shi, J. Fan, Y. Cao, Z. Peng, Y. Zhang, F. Zhu, Q. Sun, Z. Xue, Y. Liu, K. Du, Electrochim. Acta 364 (2020) 137127.
6. S.H. Lee, B.S. Jin, H.S. Kim, Sci. Rep. 9 (2019) 17541.
7. S.H. Lee, H.S. Kim, B.S. Jin, J. Alloy. Comp. 803 (2019) 1032-1036.
8. Y.K. Li, W.X. Wang, C. Wu, and J. Yang, Trans. Electr. Electron. Mater. 23 (2022) 64-71.
9. S.H. Lee, S. Lee, B.S. Jin, H.S. Kim, Sci. Rep. 9 (2019) 8901.
10. S.H. Lee, G.J. Park, S.J. Sim, B.S. Jin, H.S. Kim, J. Alloy. Comp. 791 (2019) 193-199.
11. S.H. Lee, K.Y. Kim, J.R. Yoon, NPG Asia Materials 12 (2020) 28.
12. S.H. Lee, S.J. Sim, B.S. Jin, H.S. Kim, Mater. Lett. 270 (2020) 127615.